Electron Transfer

Arylamine-Substituted Hexa-*peri*-hexabenzocoronenes: Facile Synthesis and Their Potential Applications as "Coaxial" Hole-Transport Materials**

*Jishan Wu, Martin Baumgarten, Michael G. Debije, John M. Warman, and Klaus Müllen**

Organic semiconductors for hole injection, hole transport, and photoconduction are needed in thin-film electronics, such as organic light-emitting diodes (OLEDs),[1] solar cells,[2] field-effect transistors (FET),[3] and photorefractive systems.[4] Triarylamines are particularly useful because of their ability to transport positive charge via their radical cations.[5] Hexa-*peri*-hexabenzocoronenes (HBC) have recently been introduced as discotic liquid-crystalline materials which display high charge-carrier mobility along their one-dimensional π-stacks.[6] Herein, a series of novel hole transport materials **1**–**5** is described in which HBC is peripherally substituted with arylamine moieties. They are shown to adopt a columnar stacking owing to the strong π–π interactions between the HBC cores, and thus allow charge-carrier transport by both the HBC and arylamine moieties in a coaxial supramolecular array (Scheme 1). The oxidative formation of radical cations and higher charged cations raises questions as to the intramolecular spin–spin interactions and suggests a comparison between the HBC (superbenzene) and the corresponding, much smaller benzene species.[7,8]

Our synthesis of HBC materials by oxidative cyclodehydrogenation of appropriately substituted hexaphenylbenzene precursors is not applicable owing to the radical cation formation at the nitrogen centers.[8] An alternative approach is by palladium-catalyzed Buchwald–Hartwig coupling[9] starting from the planarized HBC building blocks carrying bromo or iodo substituents. Thus, the mono- and bis- di(4-methoxyphenyl)amino-substituted HBCs (**1** and **2**) were synthesized by aryl amination between bis(4-methoxyphenyl)amine and the related mono- and dibromo HBC[10] in 65% and 76% yield, respectively (see Supporting Infor-

[*] Dr. J. Wu, Dr. M. Baumgarten, Prof. Dr. K. Müllen
Max-Planck-Institut für Polymerforschung
Ackermannweg 10, 55128 Mainz (Germany)
Fax: (+49) 6131-379-350
E-mail: muellen@mpip-mainz.mpg.de
Dr. M. G. Debije, Prof. Dr. J. M. Warman
IRI, Delft University of Technology
Mekelweg 15, 2629 JB Delft (The Netherlands)

[**] This work was financially supported by the Zentrum für Multifunktionelle Werkstoffe und Miniaturisierte Funktionseinheiten (BMBF 03N 6500), the Deutsche Forschungsgemeinschaft (Schwerpunkt Organische Feldeffekttransistoren, as well as the EU project DISCELs (G5RD-CT-2000-00321) and MAC-MES (Grd2-2000-30242).

Supporting information for this article is available on the WWW under http://www.angewandte.org or from the author.

 DOI: 10.1002/ange.200460174

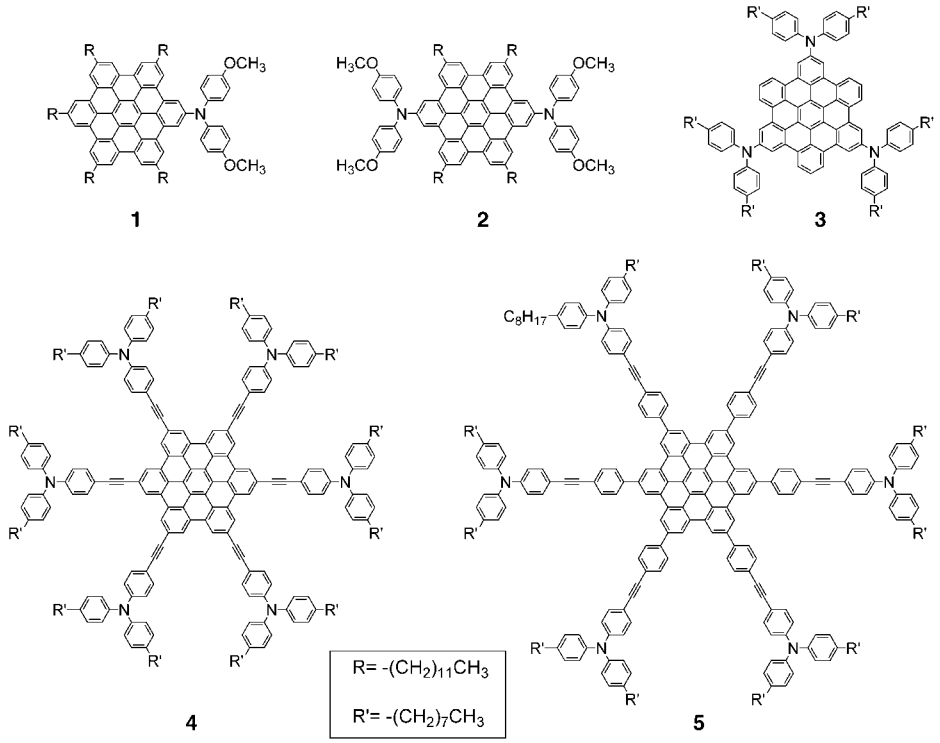

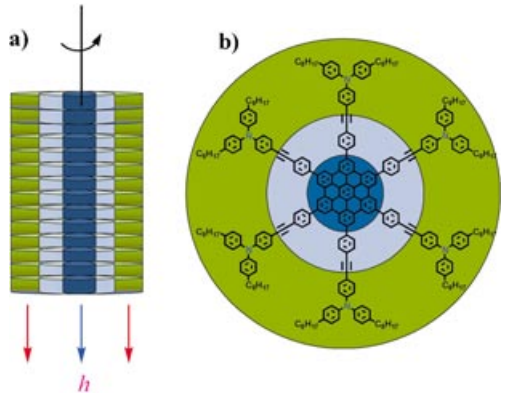

Scheme 1. Schematic presentation of a coaxial "double-cable" approach for hole transport.

mation). The synthesis of di(4-octylphenyl)amino-substituted HBC-arylamine materials (**3**–**5**) was based on a novel synthetic concept recently developed in our group.[11] A virtually insoluble HBC building block hexakis(4-iodophenyl)-*peri*-hexabenzocoronene (**6**) appeared highly reactive during the palladium catalyzed Hagihara–Sonogashira coupling reactions[12] to afford a series of soluble HBC materials which are highly ordered liquid crystals or carry electroactive substituents, such as the HBC derivative **5**. Herein, two new insoluble building blocks **7** and **8**, are introduced and utilized for the synthesis of the corresponding tris (**3**)- and hexaamines (**4**).

On route to a C_3 symmetric tris(biphenylyl)benzene precursor **14** (Scheme 2) the selective Suzuki coupling[13] between 1-bromo-2-iodobenzene (**9**) and 3-(trimethylsily)phenyl boronic acid (**10**)[14] afforded 2-bromo-3′-(trimethylsilyl)biphenyl (**11**) in 93% yield. The bromo functionality in **11** was then converted into boronic acid **12** in 90% yield, and the threefold Suzuki coupling between **12** and 1,3,5-tribromobenzene gave 1,3,5-tris[3″-(trimethylsilyl)-2′-biphenyl]benzene (**13**) in 58% yield. After replacement of the trimethylsilyl groups by iodo units (91% yield), the resulting precursor **14** was submitted to $FeCl_3$ oxidative cyclodehydrogenation conditions to give the fused HBC building block **7** as an insoluble yellow powder in 92% yield. The extremely poor solubility of compound **7** only allows solid-state MALDI-

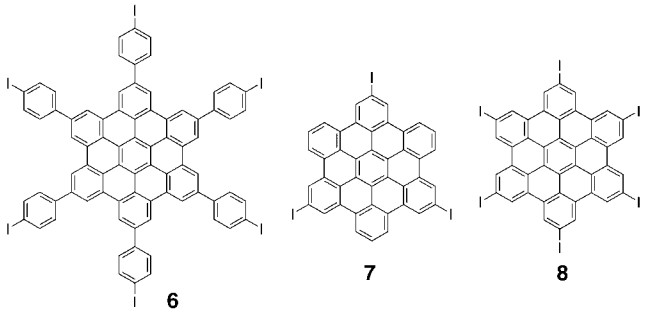

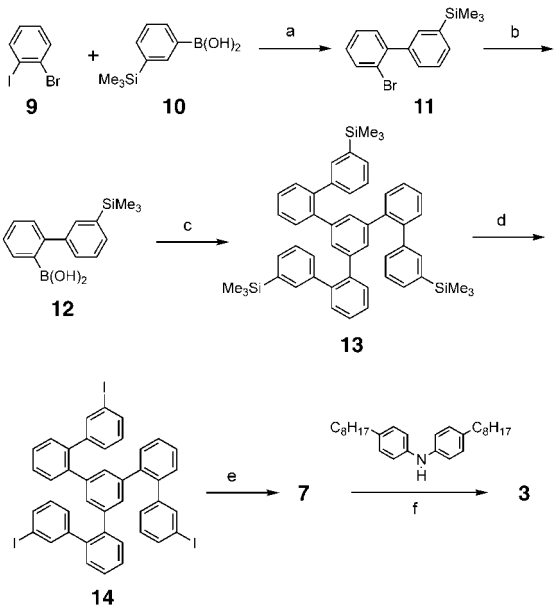

Scheme 2. Synthesis of molecule **3**: a) $[Pd(PPh_3)_4]$, K_2CO_3(aq.), toluene, 95 °C, 92%; b) 1) *n*BuLi, −78 °C; 2) $B(OCH_3)_3$, −78 °C→RT; 3) HCl (aq.), 90%; c) $[Pd(PPh_3)_4]$, K_2CO_3(aq.), toluene, 95 °C, 58%; d) ICl, chloroform, 91%; e) $FeCl_3$ (24 equiv), CH_3NO_2/CH_2Cl_2, 92%; f) $[Pd_2(dba)_3(PtBu_3)]$, toluene, 80 °C, 24%. dba = dibenzylideneacetone

TOF mass spectroscopic characterization. The subsequent functionalization of **7** with bis(4-octylphenyl)amine by Buchwald–Hartwig coupling reactions[9] afforded soluble HBC-arylamine materials **3** in 24% yield, allowing full structural characterization (see Supporting Information).

Another D_{6h} symmetric HBC, namely hexakis(4-iodo)-*peri*-hexabenzocoronene (**8**), was prepared by similar oxidative cyclodehydrogenation of the precursor hexakis(4-iodophenyl)benzene (**15**)[15] in nearly quantitative yield (see Supporting Information). Although virtually insoluble, **8** underwent sixfold Hagihara–Sonogashira coupling[12] with *N*,*N*′-bis(4-octylphenyl)-*N*″-(4-ethynylphenyl)amine (**16**) smoothly affording the soluble HBC **4** in 61% yield (Scheme 3).

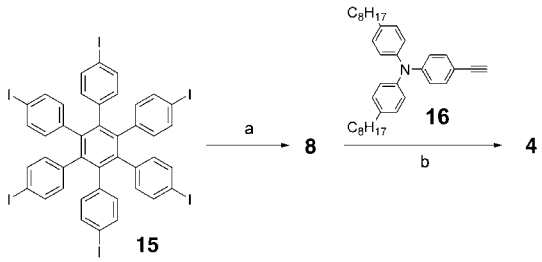

Scheme 3. Synthesis of molecule **4**: a) $FeCl_3$ (24 equiv), CH_3NO_2/CH_2Cl_2, quantitative; b) [$Pd(PPh_3)_4$]/CuI, piperidine, 50°C, 61%.

The self-assembly properties of the arylamine substituted HBCs **1**–**5** in the bulk were investigated by differential scanning calorimetry (DSC), polarized optical microscopy (POM), and two-dimensional wide-angle X-ray diffraction (2D WAXD) techniques.[16] Upon heating, **1** entered a hexagonally ordered columnar liquid-crystalline phase at 162°C, as indicated by the typical fan-type texture in POM and 2D WAXD diagrams (see Supporting Information). Upon cooling from the isotropic melt above 375°C, the compound passed through the columnar liquid-crystalline phase and gave rise to a columnar microcrystalline phase at 127°C. The typical 2D X-ray diffractogram at room temperature (Figure 1a) shows the "X" shaped reflections beyond the equatorial and meridianal directions, which are correlated to a π–π stacking distance of 4.5 Å along the stacking axis and indicate that the discs are tilted about 30° with respect to the columnar axis.[17] Similarly, upon heating, **2** entered a columnar liquid-crystalline phase at 217°C from a columnar microcrystalline phase (see POM textures and 2D WAXD measurements in Supporting Information). At room temperature there is a tilted columnar stacking of the HBC discs (Figure 1b) with an orthorhombic 2D unit cell ($a = 2.28$, $b = 1.78$ nm). A series of reflections at the wide-angle area in the equatorial and meridianal directions can be correlated to the positional or rotational order between the arylamine arms in the columnar stacking. While HBC **3** only displayed a crystalline phase bellow the melting point of 387°C, the hexaamine substituted HBCs **4** and **5** did not show any phase transition between −100°C and 400°C. The 2D WAXD measurements on the extruded fibers of **4** and **5** clearly revealed a hexagonal columnar stacking in a wide temperature range (Figure 1c). Thus, except molecule **3**, all the arylamine substituted HBCs clearly display ordered coaxial columnar stacking in the liquid-crystalline phase or microcrystalline phase; such coaxial stacking affords the opportunity of a "double-cable" hole transport (see scheme 1). At the same time, smooth thin films with thickness of tens to one hundred nanometers and roughness around 1 nm can be easily obtained for compounds **3**–**5** by spin-coating the solutions onto different substrates, such as quartz, silicon wafer, and highly oriented pyrolytic graphite (HOPG) as studied by atomic force microscope (AFM). The smooth UV/Vis absorption spectra can be obtained for these thin films. On the other hand, the thin films of compounds **1** and **2** showed typical crystalline domains on quartz mainly because of their crystalline properties at room temperature (see Supporting Information).

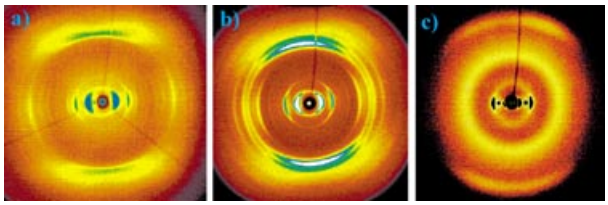

Figure 1. Representative 2D WAXD diagrams of extruded fibers of compound **1** (a), **2** (b), and **5** (c) at room temperature.

Compounds **1**–**5** can be easily oxidized to stable radical cations or higher cationic charged species, as indicated by the cyclic voltammetric and differential-pulse voltammetric measurements (Table 1 and Supporting Information). The

Table 1: Cyclic voltammetry and differential pulse voltammetry data of compound **1**–**5** in 1,2-dichlorobenzene.[a]

Event	1	2	3	4	5
$E_{1/2}^{1}$ (V)	0.47(1e)	0.34(1e)	0.51(1e)	0.77(me)	0.71(me)
$E_{1/2}^{2}$ (V)	0.94(me)	0.50(1e)	0.72(2e)	1.10(me)	0.92(me)
$E_{1/2}^{3}$ (V)	–	0.97(me)	1.23(me)	1.24(me)	1.07(me)

[a] For full details see the Supporting Information. The half-wave potential $E_{1/2}$ was refer to an $AgNO_3$/Ag reference electrode and was calibrated with an internal standard, ferrocene/ferrocenium redox system ($E_{1/2}$(Fc) = 0.232 V). 1e = one electron transfer; 2e = two electron transfer, and me = multi-electron transfer.

splitting of the oxidation of the amines in **2** and **3** into two steps (before the muli-electron event) suggests effective charge delocalization through the HBC core in the mixed-valence radical monocation species ($\mathbf{2}^{+\cdot}$ and $\mathbf{3}^{+\cdot}$). We thus monitored the Vis/NIR and electron spin resonance (ESR) spectra upon oxidative titration. The UV/Vis/NIR spectra of $\mathbf{2}^{+\cdot}$ in CH_2Cl_2 during stepwise oxidation by thianthrenium perchlorate ($THClO_4$) revealed the absorption band of a radical monocation centered 601 nm and 709 nm, together with a unique long-wavelength absorption band above 1200 nm, where the maximum peak is beyond 2200 nm (< 0.56 eV; Figure 2). The five-line ESR spectrum observed

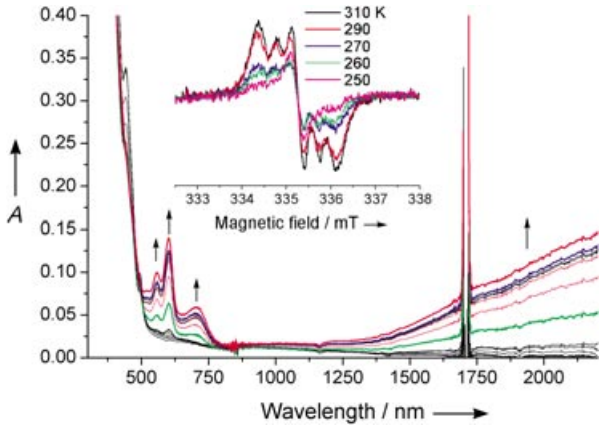

Figure 2. UV/Vis/NIR spectroscopic titration profile of compound **2** in CH_2Cl_2 with $THClO_4$ solution. Inset: temperature-dependent ESR spectra of the oxidized mono radical cation of **2**.

at 310 K for $\mathbf{2}^{+\cdot}$ reflects an intramolecular spin exchange between two nitrogen centers (Figure 2, inset). Upon going to 250 K, only a three-line signal is seen which resembles the situation found for $\mathbf{1}^{+\cdot}$.[18] Upon lowering the temperature the intensity of the ESR signals of $\mathbf{1}^{+\cdot}$ and $\mathbf{2}^{+\cdot}$ decreases, suggesting π–π aggregate formation in solution (Figure 2, inset). The long-wavelength absorption band of $\mathbf{2}^{+\cdot}$, thus can be explained by the molecular cation absorption, which is predicted to be around 1400 nm (AM1-CI calculation), and an additional intramolecular charge-transfer process. Intramolecular charge-transfer reactions in mixed-valence triarylamine systems have often been studied.[7,8,19] Herein, we provide evidence for aggregation of the radical cations of **1**–**3** even at low concentration (about 10^{-5} M) and additional intramolecular charge-transfer interactions between arylamine moieties but no clear indication could be found for the intermolecular charge transfer other than their π–π aggregation.

The intracolumnar charge-carrier mobilities for compounds **1** through **5**, determined using the pulse-radiolysis time-resolved microwave conductivity technique (PR-TRMC)[6b,20] are shown as a function of temperature in Figure 3. The mobilities are seen to differ by more than one order of magnitude, with room temperature values of 0.11, 0.21, 0.01, 0.03 and 0.04 $cm^2(Vs)^{-1}$ for **1**–**5**, respectively. The order of the mobilities for compounds **1**, **2**, and **5**, that is, **2** > **1** > **5**, are seen to be in qualitative agreement with the sharpness of the WAXD images shown in Figure 1. This supports the expected dependence of charge transport on the degree of columnar order. These largest mobility values which approach those found for the crystalline and liquid-crystalline phases of a hexadecyl-substituted HBC[6b] would be surprising if a large portion of the positive charges resided on the peripheral amine moieties: either the amines are sufficiently well-organized within the intercolumnar space to allow rapid hole transport between them, or the electrons, which remain localized on the HBC cores, have an intracolumnar mobility which is comparable with that of holes. Unfortunately the TRMC technique cannot differentiate between these two possibilities since it is insensitive to the sign of the charge of the major carrier; but the former explanation suggests that the hole mobilities in the present discotic materials are considerably larger than those found in disordered triarylamine solids.[21]

In conclusion, the new synthetic concept towards electroactive arylamine substituted HBC materials can be used to broaden the HBC family with high atom economy. Combination of the columnar superstructure formation of HBC and the hole-transporting ability of both the HBC and arylamines led to new kind of hole-transporting materials with high carrier mobility, good film formation capability (expect compound **1** and **2**), and low ionization potential, which are promising properties for organic devices.[1,2] The mixed-valence compounds of oxidized **1**–**5**, can be regarded as ideal models for studying the intramolecular charge transfer as a function of the molecular symmetry and distance between the nitrogen centers, and the intermolecular association of charged π systems.[22]

Received: March 31, 2004
Revised: June 17, 2004

Keywords: arylamines · electron transfer · hole transport · liquid crystals · pi interactions

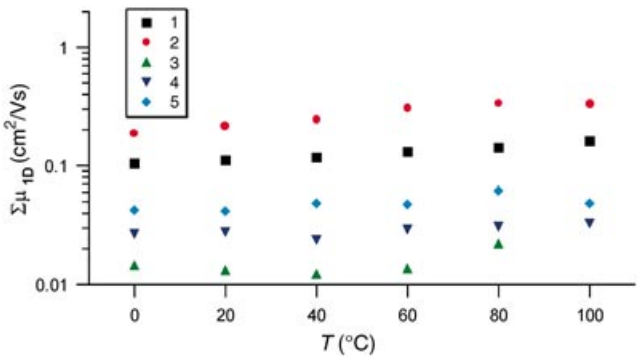

Figure 3. The temperature dependence of the one-dimensional charge-carrier mobilities of compounds **1**–**5** as measured using the PR-TRMC technique.

[1] a) C. W. Tang, S. A. VanSlyke, *Appl. Phys. Lett.* **1987**, *51*, 913–915; b) R. H. Friend, R. W. Gymer, A. B. Holmes, J. H. Burroughes, R. N. Marks, C. Taliani, D. D. C. Bradley, D. A. Dos Santos, J. L. Brédas, M. Lögdlund, W. R. Salaneck, *Nature* **1999**, *397*, 121–128.
[2] a) C. W. Tang, *Appl. Phys. Lett.* **1986**, *48*, 183–185; b) U. Bach, D. Lupo, P. Compte, J. E. Moser, F. Weissörtel, J. Salbeck, H. Spreitzer, M. Grätzel, *Nature* **1998**, *395*, 583; c) N. S. Sarififtci, L. Smilowitz, A. J. Heeger, F. Wudl, *Science* **1992**, *258*, 1474–1476.
[3] Z. Bao, J. A. Rogers, E. Katz, *J. Mater. Chem.* **1999**, *9*, 1895–1904.
[4] S. J. Zilker, *ChemPhysChem* **2000**, *1*, 72–87.
[5] M. Thelakkat, *Macromol. Mater. Eng.* **2002**, *287*, 442–461.
[6] a) M. D. Watson, A. Fechtenkötter, K. Müllen, *Chem. Rev.* **2001**, *101*, 1267–1300; b) A. M. van de Craats, J. M. Warman, A. Fechtenkötter, J. D. Brand, M. A. Harbison, K. Müllen, *Adv. Mater.* **1999**, *11*, 1469–1472.

[7] K. R. Stickley, S. C. Blackstock, *J. Am. Chem. Soc.* **1994**, *116*, 11576 – 11577.
[8] a) C. Lambert, G. Nöll, *Angew. Chem.* **1998**, *110*, 2239 – 2242; *Angew. Chem. Int. Ed.* **1998**, *37*, 2107 – 2110; b) C. Lambert, G. Nöll, *J. Am. Chem. Soc.* **1999**, *121*, 8434 – 8442; c) C. Lambert, G. Nöll, *Chem. Eur. J.* **2002**, *8*, 3467 – 3477.
[9] a) J. P. Wolfe, S. L. Buchwald, *J. Org. Chem.* **1997**, *62*, 6066 – 6068; b) J. F. Hartwig, M. Kawatsura, S. I. Hauck, K. H. Shaughnessy, L. M. Alcazar-Roman, *J. Org. Chem.* **1999**, *64*, 5575 – 5580.
[10] S. Ito, M. Wehmeier, J. D. Brand, C. Kübel, R. Epsch, J. P. Rabe, K. Müllen, *Chem. Eur. J.* **2000**, *6*, 4327 – 4342.
[11] J. Wu, M. D. Watson, K. Müllen, *Angew. Chem.* **2003**, *115*, 5487 – 5491; *Angew. Chem. Int. Ed.* **2003**, *42*, 5329 – 5333.
[12] S. Taskahashi, Y. Kuroyama, K. Sonogashira, N. Hagihara, *Synthesis* **1980**, 627 – 630.
[13] N. Miyaura, A. Suzuki, *Chem. Rev.* **1995**, *95*, 2457 – 2483.
[14] C. L. Nesloney, J. W. Kelly, *J. Org. Chem.* **1996**, *61*, 3127 – 3137.
[15] J. A. Hyatt, *Org. Prep. Proced. Int.* **1991**, *23*, 460 – 463.
[16] 2D WAXD was performed on a mechanically extruded fiber with the X-ray beam perpendicular to the fiber axis. For experimental details, see: I. Fischbach, T. Pakula, P. Minkin, A. Fechtenkötter, K. Müllen, H. W. Spiess, *J. Phys. Chem. B* **2002**, *106*, 6408 – 6418.
[17] An approximate 2D monoclinic unit cell $a = 2.17$, $b = 1.56$ nm, and $\chi = 97°$ can also be determined based on the correlations of the equatorial reflections.
[18] At low temperature the intramolecular charge transfer most probably was forbidden, thus only three-line ESR spectra correlated to singly charged amines were observed.
[19] a) J. Bonvoisin, J. P. Launay, M. van der Auweraer, F. C. De Schryver *J. Phys. Chem.* **1994**, *98*, 5052 – 5067; b) V. Coropceanu, M. Malagoli, J. M. André, J. L. Brédas, *J. Am. Chem. Soc.* **2002**, *124*, 10519 – 10530.
[20] P. G. Schouten, J. M. Warman, M. P. de Haas, *J. Phys. Chem.* **1993**, *97*, 9863 – 9870.
[21] a) P. M. Borsenberger, L. Pautmeier, R. Richert, H. Bässler, *J. Chem. Phys.* **1991**, *94*, 8276 – 8281; b) P. M. Borsenberger, L. Pautmeier, H. Bässler, *J. Chem. Phys.* **1991**, *94*, 5447 – 5454.
[22] A detailed study of the intramolecular charge transfer in the mixed-valence compounds will be presented in a separate publication.

